5-2020

Functional Analysis of a Critical Glycine (Glycine 12) in Beta-type Connexins of Human Skin

Rasheed Bailey
baileyra01@mail.buffalostate.edu

Advisor
I. Martha Skerrett, Ph.D.
First Reader
I. Martha Skerrett, Ph.D.
Second Reader
Derek L. Beahm, Ph.D.
Third Reader
Gregory J. Wadsworth, Ph.D
Department Chair
Daniel L. Potts, Ph.D.

Functional Analysis of a Critical Glycine (Glycine 12) in *Beta*-type Connexins of Human Skin

by

Rasheed Bailey

Submitted in Partial Fulfillment

of the Requirements

for the Degree of

Master of Arts

May 2020

Buffalo State College

State University of New York

Department of Biology

ABSTRACT OF THESIS

Functional Analysis of a Critical Glycine (Glycine 12) in *Beta*-type Connexins of Human Skin

At least five beta-type connexins are expressed in various layers of the skin (Cx26, Cx30, Cx30.3, Cx31, and Cx32) and all include a glycine residue at position 12. Glycine12 (G12) is located about halfway through the cytoplasmic amino terminus and has been the focus of several studies related to connexin diseases and gap junction channel structure. The importance of this residue is evident in the severity and diversity of diseases associated with amino acid substitutions at G12 including hereditary forms of skin disease, deafness and neuropathy. This study uses bioinformatic analysis in combination with mutational analysis and electrophysiology to better understand the importance of G12. Sequence alignments revealed that G12 is one of only three conserved glycine residues in beta-type connexins of skin. The functional consequences of mutations at position G12 were investigated through expression and characterization in *Xenopus* oocytes. Three disease-associated mutants were created and expressed including Cx31G12D, Cx31G12R and Cx32G12S. Cx31G12D induced cell death through a mechanism that was mildly calcium-sensitive. Cx31G12R and Cx32G12S drastically reduced the formation of functional intercellular channels. These data are consistent with other studies reporting a variety of functional consequences when G12 is altered in beta-type connexins.

Buffalo State College

State University of New York

Department of Biology

Functional Analysis of a Critical Glycine (Glycine 12) in *Beta*-type Connexins of Human Skin

A Thesis in
Biology
By

Rasheed Bailey

Submitted in Partial Fullfillment
Of the Requirements for the Degree of

Master of Arts
May 2020

Approved by

I. Martha Skerrett, Ph.D.
Professor of Biology and Chair of the Committee

Daniel Potts, Ph.D.
Associate Professor and Chair of Biology

Kevin Miller, Ed.D.
Dean of the Graduate School

Thesis Committee

I. Martha Skerrett, Ph.D.
Professor of Biology

Gregory Wadsworth, Ph.D.
Associate Professor of Biology

Derek L. Beahm, Ph.D.
Assistant Professor of Biology

Acknowledgements

I would first like to thank my mentor and friend Dr. Martha Skerrett. I've known her for almost 10 years and she has always been a pillar of support and knowledge. She became a second mother to me and without her kindness during my many rough patches I may not be where I am today. I would like to thank my committee members Dr. Gregory Wadsworth and Dr. Derek Beahm. Dr. Wadsworth is a fountain of knowledge regarding genetics and laboratory protocols. His classes provided the framework for my laboratory skills and I still follow his recommendations regarding laboratory notebook upkeep and ethics. Dr. Beahm was very patient and supportive in teaching me the jargon of electrophysiology and cell biology. His laid back mentality always kept me calm during tough times and I've tried to adopt the same outlook on life. I would also like to thank the Skerrett lab. The Skerrett lab became a family to me while I was in Buffalo and we weathered all the storms. I would like to especially thank Jamal Williams, Jesse Asiedu and Adedoyin Akingbade. The time we spent together in and out of classes were precious to me. I would also like to thank the Wadsworth lab, particularly Antonio Rockwell. I've always seen Antonio as an older brother and I aspire to reach in his successes. He pushes me to achieve my full potential. I would like to thank my family in Brooklyn with emphasis on my mother who made many sacrifices to ensure I had everything I needed to succeed. Lastly, I would like to thank Buffalo State College for accepting me into the Biology major and helping me mature into a competent scientist.

TABLE OF CONTENTS

LIST OF TABLES

LIST OF FIGURES

Introduction

Overview of Gap Junction Structure and Function

Gap junctions are gated intercellular channels that form narrow pores allowing the exchange of ions, metabolites and signaling molecules between cells (Berg *et al*., 2002). Each gap junction channel is comprised of two hemichannels (connexons) and each hemichannel involves a hexameric arrangement of subunit proteins around a central pore (Berg *et al.* 2002). The connexin family of transmembrane proteins assemble to form vertebrate gap junctions, while innexin proteins assemble to form invertebrate junctions (Lodish *et al.*, 2004). Connexins are named according to their predicted molecular weight. For example connexin31 (Cx31) has a predicted molecular weight of 31 kilodaltons while connexin26 (Cx26) has a predicted molecular weight of 26 kilodaltons (Berg *et al*., 2002).

There are 21 different human connexins encoded in the human genome (Laird, 2006). While it is it is clear that connexins are expressed in specific but overlapping patterns knowledge of their expression patterns and functions is continually being refined (Scott and Kelsell, 2011). Connexins share a common membrane topology but have unique amino acid sequences, permeability, gating patterns and sites for regulation (Harris, 2001) reflecting their diverse functions. The standard connexin topology includes four transmembrane domains (M1-M4), cytoplasmic amino and carboxyl termini, and two extracellular loops (**Figure 1).**

Each gap junction channel is composed of twelve connexins, six from one cell and six from its communicating partner. The six connexins contributed by each cell are arranged around a central pore forming a connexon, or hemichannel (**Figure 2A**). Connexon hemichannels generally

remain closed until they dock with a connexon in an adjacent cell, however physiological roles for hemichannels are being discovered each year (Goodenough and Paul, 2003).

The genes encoding connexins are classified into groups based on evolutionary origin and sequence similarity (Hsieh *et al.,* 1991). Most of the smaller connexins, for instance Cx26, Cx31 and Cx32 are grouped together as beta-type connexins (**Figure 2B)** and their gene names reflect this categorization (eg. GJB2, GJB3, and GJB1 respectively). The numbers are assigned based on the order in which the genes were identified. For instance Cx32 and Cx43 were two of the first connexins to be identified and this is reflected by the gene names GJB1 and GJA1 respectively (Willecke *et al.,* 2002).

Focus on the Amino Terminus

Of the 21 connexins in the human genome there are currently high-resolution atomic models for three: Cx26, Cx46 and Cx50 (Maeda *et al*., 2009; Bennett *et al.,* 2016; Myers *et al.,* 2018). Structural data related to Cx26 (Maeda *et al.,* 2009; Bennett *et al.,* 2016) is the best representation of beta-type connexins. A side-view of the Cx26 pore as determined by Maeda *et al*., (2009) is shown in **Figure 3.** The N-terminus (NT) is highlighted in red and can been seen lying adjacent to the channel wall, folded into the pore. This data is consistent with an earlier cryo-EM structure of a gap junction channel composed of Cx26 that revealed a "plug" in the vestibule of the channel (Oshima *et al*., 2007) lending support to the hypothesis that the NT folds into the channel. Other studies have provided information about the structure and function of the NT using site-directed mutagenesis, expression in cell lines, dye transfer assays, electrophysiology and nuclear magnetic resonance (NMR). These studies suggest that the NT is important for protein trafficking,

oligomerization and channel gating (Verselis *et al*., 1994; Purnick *et al.,* 2000[a]; Kyle *et al.,* 2008; Kalmatsky *et al.,* 2012). The N-terminus of Cx26 has also been studied as an independent peptide using nuclear magnetic resonance (Purnick *et al.*, 2000[b]). The structure revealed a flexible hinge flanked by two helical domains suggesting a "domain-hinge-domain" model of NT placement within the mouth of the pore. It was proposed that a turn involving residues 12-15 acts as the hinge, with residues 1-10 positioned in the channel entrance. Mutations that disrupt the open turn as visualized by NMR also disrupt channel function (for example, G12S, G12Y, and G12V).

Skin Disease and Mutations of the Glycine Residue G12

Connexin mutations underlie a wide range of hereditary disorders including cataracts, deafness and skin disease (Laird, 2006). Several different skin disorders are cause by connexin mutations (Mese *et al*., 2007). **Figure 4** shows a cross section of human skin identifying major layers of the skin and highlighting the beta-type connexins such as connexin26, connexin30, connexin30.3, connexin31, connexin31.1 and connexin32 (Di *et al*., 2001; Mese *et al.,* 2007). These connexins of skin are discussed below with particular focus on skin disease and point mutations occurring at G12. While mutations inducing amino acid substitution of G12 represent a small subset of the mutations associated with skin disease they occur in a number of connexins and are linked to several skin diseases **(Table 1).**

Connexin26 (GJB2) Mutations in the gene encoding connexin26 were first associated with hereditary skin disorders in 2002 when mutations in the cytoplasmic domains and first extracellular loop were associated with keratitis-ichthyosis-deafness (KID) syndrome (Richard *et al.,* 2002).

KID syndrome was first identified in 1981 by Skinner and colleagues and is a rare hereditary disorder related to development of stratifying epithelium that affects the skin and also causes sensorineural hearing loss. The gene encoding Cx26 (GJB2) was identified as a gene associated with sensorineural hearing loss (Kelsell *et al.*, 1997) with up to 50% of non-syndromic deafness cases caused by defects in GJB2 (Denoyelle *et al*., 1999). Only a subset of deafness mutations also cause skin disease. One of those mutations is G12R (Lazic *et al*., 2012) which causes symptoms of KID syndrome. In addition, the hereditary mutation Cx26G12V was associated with deafness but not skin disease when found in patients heterozygous for GJB2 mutations (Kenna *et al.*, 2001). This demonstrates that the nature of an amino acid substitution induced by a hereditary mutation can effect physiology and also highlights the importance of understanding the functional consequences of specific mutations.

Connexin30 (GJB6) Mutations in the gene encoding connexin30 are also linked to deafness and to skin disease (Bitner-Glindzic, 2002). The primary skin condition is known as Clouston syndrome, a disorder that affects hair, teeth, nails and skin (Lamartine *et al*., 2000). Thus far mutations of the glycine residue G12 have not been reported in Cx30 however mutation at an adjacent glycine (G11) is implicated in Clouston syndrome (Chen *et al.*, 2010). Glycine occurs at position 11 in only two of the beta-type skin connexins (Cx26 and Cx30) while other beta-type connexins of skin include serine at position 11 (eg. S11, G12).

Connexin30.3 (GJB4) Mutations in the gene encoding connexin30.3 are linked to the hereditary skin disease erythrokeratoderma variabilis (EKV) (Richard *et al.*, 2003) a disease characterized by transient erythema and hyperkeratosis. Palmoplantar keratoderma is present in some patients and

in most cases the phenotype is apparent within the first year of an infant's life A number of point mutations have been identified in families presenting with EKV including the missense mutation G12D (Richard *et al*., 2003; Van Steesel *et al.,* 2009).

Connexin31 (GJB3) Mutations in the gene encoding connexin31 were the first connexin mutations linked to hereditary skin disease (Richard *et al.,* 1998). Mutations in the gene encoding connexin31 have also been linked to hereditary deafness and neuropathy (Lopez-Bigas *et al.,* 2001). So far two EKV mutations have been identified at position G12 in Cx31: G12D (Rouan *et al.,* 2003) and G12R (Diestel *et al*., 2002; He *et al.,* 2005).

Connexin31.1 (GJB5) The gene encoding connexin31.1 was associated with skin physiology when it was found to be expressed in skin and inner ear (Xia *et al*., 1998). However, mutations in Cx31.1 were associated with deafness but not skin disease and no mutations have so far been identified at position G12.

Connexin32 (GJB1) Hereditary mutations in the gene encoding connexin32 were first associated with a neurodegenerative disease known as Charcot-Mare Tooth Disease (CMTX) (Bergoffen *et al.,* 1993). Charcot-Marie-Tooth disease type X (CMTX) is a demyelinating disease associated disruption of myelin. Cx32 forms channels between layers of the myelin sheath which provide a radial diffusion pathway for metabolites and nutrients. Over 160 CMTX-associated mutations in the Cx32 gene have been identified (Bone *et al.,* 1997). One of these involves an amino acid substitution at position 12 (G12S) (Bone *et al.,* 1997; Abrams *et al.,* 2001). Thus far there have

been no skin diseases associated with mutations in Cx32, likely because it is expressed at low levels and only in specific types of skin (eg. the palm, Di *et al*., 2005).

Critically Positioned Glycine

The conservation of glycine at the 12th position of beta-type connexins is speculated to play a pivotal role in channel function. Glycine is the smallest amino acid, lacking a side chain. It often facilitates turns or bends in protein structures (Marcelino and Gierasch, 2008). It was previously demonstrated by NMR that the amino terminus of connexins forms an open turn and that the turn was retained when glycine was replaced by proline but not other amino acids (eg. G12S, G12Y, G12P) (Kalmatsky *et al*., 2009). The open turn involves a reversal in the direction of the polypeptide chain. Glycine facilitates the turn based on its flexibility whereas proline induces a turn because of its cyclic structure. It was also demonstrated that of several amino acid substitutions at G12 only the G12P mutant formed functional channels (Kalmatsky *et al*., 2012).

Summary

The goal of this project was to investigate the role of G12 with focus on beta-type connexins expressed in skin. The conserved nature of G12 was examined through sequence analysis followed by a literature review of hereditary mutations at position12 in beta-type connexins of human skin. Experimental work focused on Cx31 (G12D and G12R) and Cx32 (G12S). Mutants were created using site-directed mutagenesis, RNA encoding wildtype and mutant proteins was transcribed *in vitro* and injected into *Xenopus* oocytes. Electrophysiological recordings were performed in single and paired *Xenopus* oocytes.

Methods

Sequence Analysis

Connexin sequences were obtained from Genbank (National Center for Biotechnology Information). All sequences used represent Homo Sapiens. Reference numbers, complete gene sequences, and amino acid sequences are included in **Table 2**. Amino acid sequences were aligned using MPI Bioinformatics Toolkit (Zimmerman *et al.,* 2018) specifically MAFFT software (Multiple alignment program for amino acid or nucleotide sequences (MAFFT v7; http://mafft.cbrc.jp/alignment/software/).

Creation of Mutants

The human Cx31 gene was a gift of Dr. David Kelsell (Barts and the London College of Medicine) subcloned into a *Xenopu*s oocyte expression vector by Shelby Rarick (Buffalo State Honors Thesis). The rat Cx32 gene was a gift from Dr. Bruce Nicholson (University of Texas Health Science Center at San Antonio). General features of the oocyte expression vectors are shown in **Figure 5.** Site-directed mutagenesis was performed using the Quikchange Lightning Site-Directed Mutagenesis kit (Agilent Technologies, Santa Clara, CA). The Agilent Technologies company website includes a primer design program that was used to create mutagenic primers. Mutagenic primers are typically 20 to 30 base pairs in length and incorporate single codon changes, being complementary to the gene sequence in the target region but incorporating changes necessary to substitute a single amino acid. For mutagenesis both forward and reverse primers are required, and they are complementary to one another. Primers were ordered from IDT (Integrated DNA Technologies, Newark NJ). Mutagenesis reactions were placed in a thermocycler and programmed to 18 cycles with temperatures for denaturing (98 °C), annealing (50°C) and

elongation (74°C). The final step of mutagenesis involves addition of a restriction enzyme, DpnI, to digest parental DNA. After digestion of parental DNA it is expected that most remaining plasmids contains the desired mutation. However each plasmid has the potential to be either parental (nonmutated DNA), mutated (mutation) or neither (a PCR-based error). DNA must therefore be sequenced. Prior to sequencing, the Dpn1-digested plasmid DNA is used to transform competent cells, which are grown overnight on the selective media. The following transformation procedure was used: Two microliters of the digested plasmid DNA will be added to 50 microliters of XL-1 supercompetent cells for the transformation reaction. The reaction was incubated on ice for 30 minutes then heat pulsed at 42 °C for 45 seconds and then placed on ice again for 2 minutes. A specialized S.O.C broth (2% tryptone, 0.5% yeast extract, 10 mM NaCl, 2.5 mM KCl, 10 mM MgCl2, 10 mM MgSO4, and 20 mM glucose) was added to the reaction and then incubated for 1 hour in a shaking incubator at 220 rpm. After the incubation, the transformed bacteria was plated on LB + AMP plates. One liter of LB + AMP was prepared using 20 g bacto-tryptone, 5 g yeast extract, 10 g NaCl, 100 µg/ml ampicillin. Plates included 1% bactoagar.) Plates were incubated at 37 °C overnight. The following day, colonies were selected, each colony representing one of the three possible types of plasmid. Three or four colonies were selected, used to inoculate growth media (LB+ AMP) and grown overnight for amplification. A 1.5% agarose gel was run at 75 V and stained with ethidium bromide to confirm the presence of plasmid DNA prior to sequence analysis. The DNA was compared to a DNA ladder (Zip Ruler1, Fermentas Inc.) The following day plasmid DNA was isolated using a Qiagen SpinPrep Kit (Qiagen Inc, Redwood City CA) and sent to Genscript USA (Piscataway NJ) after using gel electrophoresis to confirm quantity and quality of the DNA. Of the total 50 µl eluted in the final step of plasmid isolation, 10 µl was sent for sequence analysis. The remaining DNA was stored at -20 ° C.

The promoter for RNA polymerase varied for different constructs and the information is summarized in **Table 3.** These promoters also served as the priming sites for sequencing using Genscript's in-house primers. Genes were sequenced through all or most of the coding region Once a sequence was retrieved it was translated and the amino acid sequence was compared to the wild-type amino acid sequence to confirm both the mutation and the remaining sequence.

***In vitro* transcription.**

Prior to *in vitro* transcription plasmid DNA were linearized using restriction enzymes. Restriction enzymes were construct-specific and are summarized in **Table 3**. Linearized DNA was precipitated using 0.5 M EDTA, ethanol and sodium acetate. DNA was precipitated in a microfuge tube at -20°C for approximately 24 hours. Then the precipitate was centrifuged for 30 minutes at 13,000 rpm and DNA was suspended in 6µl nuclease-free water. The linearized DNA was analyzed by gel electrophoresis on a 1% agarose gel. The mMessage mMachine *In Vitro* Transcription Kit (Thermofisher, Grand Island, NY) was used to create RNA. Reactions included 10 µl Nucleotide Mix, 2 µl RNA polymerase, 8 µl template DNA and 2.2 µl reaction buffer. Reactions were incubated at 37°C for 2 hours. Following incubation, the RNA was precipitated using the LiCl method. This involved adding 20 µl nuclease free water and 50 µl of LiCl to the reaction and incubated overnight at -20°C. The following day the samples were centrifuged at 13,000 rpm in a 4 °C centrifuge for 20 minutes. A small RNA pellet was often apparent. It was washed with 70% ethanol and then resuspended in 10 µl of nuclease free water. Resuspended RNA was analyzed by gel electrophoresis to confirm quality and quantity. 1µl of RNA was combined with loading dye and run alongside an RNA control (Control 250 Ambion Inc.) on a 1% agarose gel for 15 minutes at 100 volts to estimate concentration (125 ng/µl).

Handling and Injection of Oocytes

Xenopus oocytes were used as an expression system to compare the characteristic of wildtype and mutated connexins. Surgical removal of oocytes from female *Xenopus laevis* frogs was conducted following a Buffalo State IACUC-approved protocol. After removal, oocytes were placed in OR2 solution (82.5 mM NaCl, 2 mM KCl, 1 mM MgCl2, 5 mM Tris base, pH 7. 20 supplemented with 20 mg/ml of streptomycin sulfate, penicillin G, and gentamicin sulfate (Sigma Chemical, St. Louis, MO). The frog was sutured and placed in shallow water to recover. The follicle layer surrounding the oocytes was partially digested using Type 1A collagenase (Sigma Chemical, St. Louis MO), typically about 70 mg dissolved in 10 ml of OR2 for 20 minutes with continuous rocking. The collagenase was removed by washing several times with fresh OR2 media before the oocytes were placed in MB1 media (88 nM NaCl, 1 mM KCl, 0.41 mM CaCl2 0.82 mM, 1 mM MgCl2, 2.4 mM NaHCO3, 0.33 mM $Ca(NO_3)2$, 20 mM HEPES pH 7.4 with NaOH, supplemented with 20 mg/ml of streptomycin sulfate, penicillin G, and gentamicin sulfate (antibiotics from Sigma Chemical, St. Louis, MO)

Injection and Recording from *Xenopus* Oocytes

Any remaining follicle layer was manually removed with fine forceps before oocytes were injected with 0.5 ng of antisense oligonucleotide directed against XeCx38 to eliminate endogenous *Xenopus* connexins (Genetools Inc, Philamel, OR). The following day RNA encoding the connexin of interest was injected (5 ng per oocyte, 41 nl volume unless otherwise stated). For recordings from single oocytes, the vitelline layer was retained and recordings were performed the following day. For intercellular recordings from paired oocytes, the vitelline layer was removed 12-24 hours after injection and the oocytes were paired together in shallow agar wells. A typical

voltage clamp experiment involving single cells involved measurement of currents while the oocyte was maintained at -40 mV between pulses to more positive and negative membrane potentials. A typical voltage clamp experiment involving paired oocytes involved continuous clamping of one cell at -20 mV while its partner is pulsed to induce transjunctional voltages of ±100 mV. Example output from four channels during a dual cell voltage clamp experiment is shown in **Figure 6**. The current measured in the clamped cells is the junctional current.

Survivorship Assays

In some cases a survivorship experiment was conducted to measure the health of oocytes over time. Oocytes were injected with RNA diluted to 75 ng/ul or 125 ng/µl and placed in a petri dish filled with solution. Three treatment solutions were used: MB1, MB1 + 2 mM $CaCl_2$ and MB1+ 1mM $CoCl_2$. Oocytes were monitored every 4 to 8 hours for changes in phenotype at whch time they were scored as healthy (no change from uninjected appearance), dying (blotchy and/or overly turgid), or dead (ruptured).

Data Analysis and Presentation

Survivorship data was analyzed and plotted using Microsoft Excel A line graph was created to view the time-dependent changes in the number of healthy oocytes. Voltage-clamp recordings were analyzed using Clampfit software (Molecular Devices, San Jose, CA) and Origin Software (OriginLab Corporation, Northampton, MA). Intercellular currents were displayed as current traces resulting from 10 mV voltage pules. Single oocyte recordings were presented in plots of current-versus voltage (I-V curves) using Origin Software (OriginLab Corporation, Northampton, MA).

Results

Amino Acid Alignments

The amino acid sequences of five *beta*-type connexins expressed in human skin were obtained from NCBI and aligned using Clustal (MPI Bioinformatics Toolkit). The alignment revealed the conserved glycine at position 12 as well as two other conserved glycine residues **(Figure 7).** G12 is located about halfway through the amino terminus while the two other conserved glycines are located in the extracellular loops.

Diseases Associated with Mutations at G12

The importance of G12 in gap junction channels is demonstrated by the number of mutations at this site associated with genetic diseases. **Table 1** shows a summary of G12 mutations in the five beta-type connexins examined in this study and the diseases associated with them. Thus far mutations at G12 have been identified in three of the beta-type connexins, Cx26, Cx30.3 and Cx31. Interestingly they cause slightly different skin disorders, and one of the Cx26 mutations (G12V) does not cause skin disease but causes deafness.

Cx31G12D Induces Cell Death

The first mutant to be created and tested in oocytes was Cx31G12D. During the first couple of attempts to test gap junction function it was noticed that oocytes injected with RNA encoding Cx31G12D were susceptible to loss of polarization followed by bursting or rupturing. To demonstrate this experimentally oocytes were observed for 72 hours and the percentage of surviving oocytes was plotted **(Figure 8).** Two different concentrations of RNA (for both mutant

and wildtype) were injected into oocytes. These were referred to as full strength RNA (125 ng/µl ≈ 5 ng/oocyte) and half strength (67 ng/µl ≈ 2.5 ng/oocyte). Oocytes were more robust after injection of HS- RNA in both cases. Oocytes injected with FS wildtype Cx31 and Cx31G12D had poor health shown by loss of pigmentation in the animal pole. Twenty-five hours after injection 100% of oligo-injected oocytes were healthy but only 50% of those injected with FS Cx31 and 70% of those injected with HS Cx31 were healthy. In the G12D group only a fraction of oocytes remained healthy after injection of HS and FS RNA respectively. The detrimental effect of connexin RNA was mildly alleviated by the addition of calcium or cobalt to the media. Media bathing the oocytes included MBI alone or supplemented with calcium ($CaCl_2$, 2 mM) and cobalt ($CoCl_2$, 1 mM). The greatest effect of divalent cations was observed with Cx31 where addition of 1 mM $CoCl_2$ improved survival at 25 hours to 100% in the HS group. In the G12D group addition of 1 mM $CoCl_2$ improved survival at 25 hours from 20% to 40% in the HS group.

Cx31G12D induces leak currents in single oocytes

To further assess the mechanism by which Cx31G12D induced cell death two-electrode voltage clamp was used assess membrane currents in single oocytes. Other skin disease mutations (in connexins) induce leaky membranes after expression in oocytes and it is hypothesized that alteration of gating of single hemichannels may underlie this behavior (Gerido *et al.*, 2007; Ambrosi *et al*., 2013). Since hemichannels are blocked by divalent cations, addition of calcium (or cobalt) is one method of testing the leaky hemichannel hypothesis. It is also possible to add gap junction blockers such as carbenoxolone. After applying a series of voltage pulses to clamped oocytes we observed that oocytes expressing Cx31G12D had larger transmembrane currents than oocytes injected with wtCx31 **(Figure 9).** Combined with the observations that addition of low

concentrations of divalent cations such as 1 mM $CaCl_2$ enhance survival there is good support for a leaky hemichannel mechanism in Cx31G12D.

Cx31G12R and Cx32G12S Induce Small Junctional Currents

Recording currents from paired oocytes, especially oocytes expressing mutants that are detrimental to cell health is challenging. However recordings were obtained for two of the G12 mutants, Cx31G12R and Cx32G12S. Oocytes expressing the mutants exhibited much smaller transjunctional currents than oocytes expressing wildtype connexin **(Figure 10; Figure 11).** These results are consistent with observations that the mutants display trafficking defects because only a small percentage of protein may traffic to the plasma membrane resulting in low levels of coupling. In terms of junctional currents the Cx31G12R pairings had much lower conductance than those from Cx31 (Cx31 WT= 37 µS, Cx31G12R=0.5 µS) and the Cx32G12S pairings had much lower conductance than those from Cx32 (Cx32 WT= 17 µS, Cx32 G12S=0.6 µS)

Discussion

After retrieving and translating human connexin sequences retrieved from GenBank,(National Center for Biotechnology Information, see Table 2) amino acid alignments were used to confirm that glycine is conservatively positioned as the twelfth amino acid within the beta-type connexins of skin. A detailed literature review revealed that a number of diseases result from amino acid substitutions at position G12 with the following mutations so far identified: Cx26G12R (Lazic *et al.,* 2012; Garcia *et al.,* 2016; Taki *et al,* 2018), Cx30.3G12D (van Steensel *et al.,* 2009), Cx31G12D (Rouan *et al*., 2003), Cx31G12R (He *et al.,* 2005), Cx32G12S (Bergoffen *et al.,* 1993; Deng *et al.,* 2019). In summary, amino acid substitutions at glycine 12 result in skin abnormalities when they occur in Cx26, Cx30.3, Cx31 or Cx32.

There has been considerable interest in understanding the role of glycine12 in channel function.. High resolution gap junction structures depict the N-terminus folded into the cytoplasmic mouth of the channel (Oshima *et al.,* 2007; Maeda *et al.,* 2009; Villenelo *et al.,* 2017). In all cases an N-terminus bend occurs near or at twelfth residue (Figure 3, Maeda *et al.,* 2009). Although it is theorized that amino acid substitutions at position 12 disrupt gap junction function, specific the structural and functional consequences of the mutations warrant further investigation. Studies using NMR to investigate structure of the N-terminus as an independent molecule indicate that the consequences of amino acid substitutions are dependent on both the connexin and the amino acid substitution (Purnick *et al.,* 2000[b]; Kalmatsky *et al.,* 2012; Batir *et al.,* 2016). For instance Cx26G12R induces a more flexible bend in the NT whereas Cx32G12R creates a more constricted turn. Functionally Cx26G12R appears to induce leaky channels whereas Cx32G12R fails to form functional channels (Batier *et al.,* 2016). In expression studies Cx31G12D trafficked to the

membrane but failed to form functional gap junction channels in HeLa cells (assessed with Flag tagged Cx31; Rouan *et al.,* 2003). Other studies showed that the Cx32G12S mutants fail to reach the plasma membrane but are trapped in the Golgi apparatus (Martin *et al.* 2000).

Mutations that disrupt channel function may do so at the level of expression, translation, trafficking, oligomerization, docking, gating, or permeability. Expression and analysis of individual mutants aims to advance understanding of the outcome and often sheds light on the link between a genetic alteration and a physiological disorders. In some cases, such as CFTR, a highly studied chloride channel linked to cystic fibrosis, treatments are tailored to specific mutations (Lopes-Pacheco, 2020). Progress is being made in understanding the mechanisms by which connexin mutations cause skin disease, particularly for two of the more highly characterized connexins, Cx26 and Cx31. Some studies report that EKV mutations, including G12D and G12R cause cell death and/or alter cell proliferation (Lee *et al.*, 2009; Taki *et al*., 2018) while others report changes in interactions between connexins (Richard *et al.* 2003). Mutations that cause cell death require more detailed characterization because they could do so by any number of mechanisms. It is possible that disrupting gating mechanisms could result in hemichannels that disrupt ion gradients. Gating disruptions could also reflect altered sensitivity to voltage, calcium, pH or phosphorylation (Harris, 2001). It is also possible that altered gating could result in channels that dock, forming gap junction channels, but with altered behavior that restricts cell communication. Hence, detailed characterization, using several techniques in a number of different expression settings usually required for correct characterization.

Fully formed gap junction channels close in response to transjunctional voltage (Vj) and each connexin has a characteristic response to Vj (Harris, 2001). It has previously been shown that charged residues in the N-terminus influence the polarity to which connexins respond (Purnik *et al*., 2000[a]). However it is not known whether other structural components influence the extent of closure in response to Vj, or the voltage to which a response is initiated. Our results do not suggest a role for G12 in gap junction channel gating, and thus far there have not been any published results that support this. However it could be argued that a disruption in the membrane potential is suggestive of altered hemichannel behavior, possibly supporting a role for G12 in channel regulation (gating).

In our study the mutant Cx31G12D induced cell death through a mechanism that appeared to involve leaky membranes. Oocytes expressing Cx31 and Cx31G12D were partially rescued by including 1 mM $CoCl_2$ or 2 mM $CaCl_2$ in the external media suggesting that leaky hemichannels may be responsible. It has been shown that some Cx26 mutants interact with Cx43 when it is coexpressed in the same cells and influence gating of Cx43 hemichannels (Shuja *et al*., 2016). It is possible that Cx31G12D is interacting with an endogenous *Xenopus* connexin although unlikely that XeCx38 is involved since oocytes were injected with morpholino antisense to silence the endogenous Cx38. In an EKV study, investigators transfected Cx31 and mutants in fibroblast cell lines (NEB1) found that all of the EKV mutants resulted in cell death and among these mutants were G12R and G12S (Di *et al*. 2005). Recent studies (Lee *et al.,* 2009, Garcia *et al*., 2018; Taki *et al.,* 2018) suggest that Cx26G12R causes leaky hemichannels potentially explaining its role in skin pathology. A recent hypothesis regarding association of Cx26 mutations with skin disease and deafness is based on the observation that some mutations induce hemichannel activity. These

mutations appear to be “gain of function” mutations that cause calcium dysregulation leading to skin disease (Shuja *et al.,* 2016). It is also worth noting that although mutations of G12 have not been reported in Cx30, mutation at an adjacent glycine (G11) is implicated in Clouston syndrome (Lamartine *et al.,* 2000).

Functional analysis has provided a link between connexin function and skin disease and has facilitated generation of several hypotheses regarding connexin function in normal and diseased skin. For instance, Cx31 is expressed in the stratum granulosum, which is comprised of granular cells containing keratohyalin granules. At the transition state between stratum granulosum and the stratum corneum, granular cells lose their nuclei and organelles and the cells become new corneocytes (Ovaere *et al*. 2009). I hypothesize that Cx31 is a key factor in the transition between granular cells and corneocytes. It is possible that granular cells receive a signal to lose their nuclei and organelles by means of autocrine or paracrine pathways or via direct communication. One protein that potentially regulates this is Cx31. Perhaps the red thickened phenotype of EKV may result from granular cells failing to become corneocytes. This hypothesis is worthy of further investigation especially promising is the concept that an ointment stimulating gap junction intercellular communication could compel the granular cells to become corneocytes..

References

Abrams CK, Freidin MM, Verselis VK, Bennett MV, Bargiello TA. 2001. Functional alterations in gap junction channels formed by mutant forms of connexin 32: evidence for loss of function as a pathogenic mechanism in the X-linked form of Charcot-Marie-Tooth disease. Brain Res. 900: 9-25.

Ambrosi C, Walker AE, Depriest AD, Cone AC, Lu C, Badger J, Skerrett IM, Sosinsky GE. 2013. Analysis of trafficking, stability and function of human connexin 26 gap junction channels with deafness-causing mutations in the fourth transmembrane helix. PLoS One. 15: 8(8):e70916.

Batir Y, Bargiello TA, Dowd TL. 2016. Structural studies of N-terminal mutants of Connexin 26 and Connexin 32 using (1)H NMR spectroscopy. Arch Biochem Biophys 608: 8-19.

Bennett BC, Purdy MD, Baker KA, Acharya C, McIntire WE, Stevens RC, Zhang Q, Harris AL, Abagyan R, Yeager M. 2016. An electrostatic mechanism for Ca(2+)-mediated regulation of gap junction channels. Nat Commun 7: 8770

Berg JM, Tymoczko JL, Stryer L. 2002. Biochemistry. 5th edition. New York: W H Freeman. Section 13.6, Gap junctions allow ions and small molecules to flow between communicating cells.

Bergoffen J, Scherer SS, Wang S, Scott MO, Bone LJ, Paul DL, Chen K, Lensch MW, Chance PF, Fischbeck KH. 1993. Connexin mutations in X-linked Charcot-Marie-Tooth disease. Science 262: 2039-2042.

Bitner-Glindzicz, M. 2002. Hereditary deafness and phenotyping in humans. Br. Med. Bull. 63: 73–94.

Bone LJ, Deschenes SM, Balice-Gordon RJ, Fischbeck KH, Scherer SS. 1997. Connexin32 and X-linked Charcot–Marie–Tooth Disease. Neurobiol of Disease 4: 221–230.

Bosco D, Haefliger J, Meda PD. 2011. Connexins: key mediators of endocrine function. Physiological Rev. 91: 1393-445.

Chen N, Xu C, Han B, Wang Z Y, Song Y L, Li S, Zhang,R L, Pan C M, Zhang L. 2010. G11R mutation in GJB6 gene causes hidrotic ectodermal dysplasia involving only hair and nails in a Chinese family. J. Dermatol. 37: 559–561.

D'Andrea P, Veronesi V, Bicego M, Melchionda S, Zelante L, Di Iorio E, Bruzzone R, Gasparini P. 2002. Hearing loss: frequency and functional studies of the most common connexin26 alleles. Biochem Biophys Res Commun. 296: 685–691.

Deng Y, Wang H, Mou Y, Zeng Q, Xiong X. 2019. Exome sequencing identifies novel compound heterozygous mutations in GJB3 gene that cause erythrokeratodermia variabilis et progressiva. Australas J Dermatol 60:e87-e89.

Denoyelle F, Marlin S, Weil D, Moatti L, Chauvin P, Garabédian EN, Petit C.1999. Clinical features of the prevalent form of childhood deafness, DFNB1, due to a connexin-26 gene defect: implications for genetic counselling. Lancet 353:1298-1303.

Di WL, Gu Y, Common JE, Aasen T, O'Toole EA, Kelsell DP, Zicha D. 2005. Connexin interaction patterns in keratinocytes revealed morphologically and by FRET analysis. J Cell Sci: 118: 1505-1514.

Diestel S, Richard G, Doring B, Traub O. 2002. Expression of a connexin31 mutation causing erythrokeratodermia variabilis is lethal for HeLa cells. Biochem Biophys Res Commun, 296: 721-728.

García IE, Maripillán J, Jara O, Ceriani R, Palacios-Muñoz A, Ramachandran J, Olivero P, Perez-Acle T, González C, Sáez JC, Contreras JE, Martínez AD. 2015. Keratitis-ichthyosis-deafness syndrome-associated Cx26 mutants produce nonfunctional gap junctions but hyperactive hemichannels when co-expressed with wild type Cx43. J Invest Dermatol 135:1338-1347.

García IE, Bosen F, Mujica P, Pupo A, Flores-Muñoz C, Jara O, González C, Willecke K, Martínez AD. 2016. From hyperactive connexin26 hemichannels to impairments in epidermal calcium gradient and permeability barrier in the keratitis-ichthyosis-deafness syndrome. J Invest Dermatol. 136:574-583.

Gerido DA, DeRosa AM, Richard G, White TW. 2007. Aberrant hemichannel properties of Cx26 mutations causing skin disease and deafness. Am J Physiol Cell Physiol 293: C337-45.

Goodenough DA, Paul DL. 2003. Beyond the gap: functions of unpaired connexon channels. Nat Rev Mol Cell Bio 4: 285-294.

Harris, AL. 2001. Emerging issues of connexin channels: biophysics fills the gap. Q Rev Biophys 34: 325-472.

He LQ, Liu Y, Cai F, Tan ZP, Pan Q, Liang DS, Long ZG, Wu LQ, Huang LQ, Dai HP, Xia K, Xia JH, Zhang ZH. 2005. Intracellular distribution, assembly and effect of disease-associated connexin 31 mutants in HeLa cells. Acta Biochim Biophys Sin 37: 547-554.

Hsieh CL, Kumar NM, Gilula NB, Francke U. 1991 Distribution of genes for gap junction membrane channel proteins on human and mouse chromosomes. Somatic Cell Molec Genet 17: 191-200.

Kalmatsky BD, Bhagan S, Tang Q, Bargiello TA, Dowd TL. 2009. Structural studies of the N-terminus of Connexin 32 using 1H NMR spectroscopy. Arch Biochem Biophys 490: 9-16.

Kalmatsky BD, Batir Y, Bargiello TA, Dowd TL. 2012. Structural studies of N-terminal mutants of connexin 32 using (1)H NMR spectroscopy. Arch Biochem Biophys 526: 1-8.

Kelsell DP, Dunlop J, Stevens HP, Lench NJ, Liang JN, Parry G, Mueller RF, Leigh IM. 1997. Connexin 26 mutations in hereditary non-syndromic sensorineural deafness. Nature 387: 80-83.

Kenna MA, Wu B, Cotanche DA, Korf BR, Rehm HL. 2001. Connexin26 studies in patients with sensorineural hearing loss. Arch Otolaryngol Head Neck Surg 127: 1037–1042.

Kyle JW, Minogue PJ, Thomas BC, Domowicz DA, Berthoud VM, Hanck DA, Beyer EC. 2008. An intact connexin N-terminus is required for function but not gap junction formation. J Cell Sci 121: 2744-2750.

Laird DW. 2006. Life cycle of connexins in health and disease. Biochem J 394:527-543.

Lamartine J, Laoudj D, Blanchet-Bardon C, Kibar Z, Soularue P, Ridoux V, Dubertret L, Rouleau GA, Waksman G. 2000. Refined localization of the gene for Clouston syndrome (hidrotic ectodermal dysplasia) in a large French family. Br J Dermatol 142: 248-252.

Lazic T, Li Q, Frank M, Uitto J, Zhou LH. 2012. Extending the phenotypic spectrum of keratitis-ichthyosis-deafness syndrome: report of a patient with GJB2 (G12R) Connexin 26 mutation and unusual clinical findings. Pediatr Dermatol 29: 349-357.

Lee JR, Derosa AM, White TW. 2009. Connexin mutations causing skin disease and deafness increase hemichannel activity and cell death when expressed in Xenopus oocytes. J Invest Dermatol 129: 870-878.

Lodish H, Berk A, Zipursky SL, Matsudaira P, Baltimore D and Darnell J. 2004 *Molecular Cell Biology* W H Freeman 5th ed. New York, NY USA.

Lopez-Bigas N, Olive M, Rabionet R, Ben-David O, Martinez-Matos JA, Bravo O, Banchs I. Volpini V, Gasparini P, Avraham KB, Ferrer I, Arbonés ML, Estivill X. 2001. Connexin 31 (GJB3) is expressed in the peripheral and auditory nerves and causes neuropathy and hearing impairment. Hum Mol Genet 10: 947-952.

Lopes-Pacheco M. 2020. CFTR Modulators: The Changing Face of Cystic Fibrosis in the Era of Precision Medicine. Front Pharmacol 10:1662.

Maeda S, Nakagawa S, Suga M, Yamashita E, Oshima A, Fujiyoshi Y, Tsukihara T. 2009. Structure of the connexin 26 gap junction channel at 3.5 A resolution. Nature 458: 597-602.

Marcelino, AM, Gierasch, LM. 2008. Roles of beta-turns in protein folding: from peptide models to protein engineering. Biopolymers 89: 380–391.

Martin PE, Mambetisaeva ET, Archer DA, George CH, Evans WH. 2000. Analysis of gap junction assembly using mutated connexins detected in Charcot-Marie-Tooth X-linked disease. J Neurochem 74: 711-720.

Mese G, Richard G, White TW. 2007. Gap Junctions: Basic Structure and Function. J Investig Dermatol 127: 2516–2524.

Myers JB, Haddad BG, O'Neill SE, Chorev DS, Yoshioka CC, Robinson CV, Zuckerman DM, Reichow SL. 2018. Structure of native lens connexin 46/50 intercellular channels by cryo-EM. Nature 564: 372-377.

Oshima A, Tani K, Hiroaki Y, Fujiyoshi Y, Sosinsky GE. 2007. Three-dimensional structure of a human connexin26 gap junction channel reveals a plug in the vestibule. Proc Natl Acad Sci USA 104: 10034-10039.

Ovaere P, Lippens S, Vandenabeele P, Declercq W. 2009. The emerging roles of serine protease cascades in the epidermis. Trends in Biochem Sci 34: 453–463.

Purnick PE, Oh S, Abrams CK, Verselis VK, Bargiello TA. 2000[a] Reversal of the gating polarity of gap junctions by negative charge substitutions in the N-terminus of connexin 32. Biophys J 79: 2403-2415.

Purnick PE, Benjamin DC, Verselis VK, Bargiello TA, Dowd TL. 2000[b]. Structure of the amino terminus of a gap junction protein. Arch Biochem Biophys 381: 181-190.

Richard G, Smith LE, Bailey RA, Itin P, Hohl D, Epstein EH Jr, DiGiovanna JJ, Compton JG, Bale SJ. 1998. Mutations in the human connexin gene GJB3 cause erythrokeratodermia variabilis. Nat Genet 20: 366-369.

Richard G, Rouan F, Willoughby CE, Brown N, Chung P, Ryynanen M, Jabs EW, Bale SJ, DiGiovanna JJ, Uitto J, Russell L. 2002. Missense mutations in GJB2 encoding connexin-26 cause the ectodermal dysplasia keratitis-ichthyosis-deafness syndrome. Am J Hum Genet 70:1341-1348.

Richard G, Brown N, Rouan F, Van der Schroeff JG, Bijlsma E, Eichenfield LF, Sybert VP, Greer KE, Hogan P, Campanelli C, Compton JG, Bale SJ, DiGiovanna JJ, Uitto J. 2003. Genetic heterogeneity in erythrokeratodermia variabilis: novel mutations in the connexin gene GJB4 (Cx30.3) and genotype-phenotype correlations. J Invest Dermatol 120: 601-609.

Rouan F, Lo CW, Fertala A, Wahl M, Jost M, Rodeck U, Uitto J, Richard G. 2003. Divergent effects of two sequence variants of GJB3 (G12D and R32W) on the function of connexin 31 in vitro. Exp Dermatol 12: 191-197.

Saez, JC, Berthoud, VM, Branes, MC, Martinez, AD, Beyer, EC 2003. Plasma membrane channels formed by connexins: Their Regulation and Functions. Physiol Rev 83: 1359-1400.

Shuja Z, Li L, Gupta S, Meşe G, White TW. 2016. Connexin26 mutations causing palmoplanta keratoderma and deafness interact with Connexin43, modifying gap junction and hemichannel properties. J Invest Dermatol 136: 225-235.

Scott CA, and Kelsell DP. 2011 Key functions for gap junctions in skin and hearing. Biochem J 438: 245-254.

Skinner BA, Greist MC, Norins AL. 1981. The keratitis, ichthyosis, and deafness (KID) syndrome. Arch Dermatol 117:285-289.

Taki T, Takeichi T, Sugiura K, Akiyama M. 2018. Roles of aberrant hemichannel activities due to mutant connexin26 in the pathogenesis of KID syndrome. Sci Rep 8: 12824.

van Steensel MA, Oranje AP, van der Schroeff JG, Wagner A, van Geel M. 2009. The missense mutation G12D in connexin30.3 can cause both erythrokeratodermia variabilis of Mendes da Costa and progressive symmetric erythrokeratodermia of Gottron. Am J Med Genet 149A: 657-661.

Verselis VK, Ginter CS, Bargiello TA. 1994. Opposite voltage gating polarities of two closely related connexins. Nature 368: 348-351.

Villanelo F, Escalona Y, Pareja-Barrueto C, Garate JA, Skerrett IM, Perez-Acle T. 2017. Accessing gap-junction channel structure-function relationships through molecular modeling and simulations. BMC Cell Biol 18: 5.

Willecke K, Eiberger J, Degen J, Eckardt D, Romualdi A, Güldenagel M, Deutsch U, Söhl G. 2002. Structural and functional diversity of connexin genes in the mouse and human genome. Biol Chem. 383: 725–377.

Xia JH, Liu CY, Tang BS, Pan Q, Huang L, Dai HP, Zhang BR, Xie W, Hu DX, Zheng D, Shi XL, Wang DA, Xia K, Yu KP, Liao XD, Feng Y, Yang YF, Xiao JY, Xie DH, Huang JZ. 1998. Mutations in the gene encoding gap junction protein beta-3 associated with autosomal dominant hearing impairment. Nat Genet 20: 270-370.

Zimmermann L, Stephens A, Nam SZ, Rau D, Kübler J, Lozajic M, Gabler F, Söding J, Lupas AN, Alva V. 2018. A completely reimplemented MPI Bioinformatics Toolkit with a new HHpred server at its core. J Mol Biol 430: 2237-2243.

TABLES

Table 1. Hereditary Mutations Involving Glycine 12 of Beta-Type Connexins

Connexin	Mutation	Hereditary Disease	References
Cx26	G12V	Deafness (non syndromic)	Kenna *et al.*, 2001; D'Andrea *et al.*, 2002 Garcia *et al.*, 2015
	G12R	Keratitis, ichthyosis and deafness (KID) syndrome	Garcia *et al*, 2015; Taki et al, 2018; Lee *et al.*, 2009; Lazic *et al.*, 2012.
Cx30.3	G12D	Erythrokeratodermia variabilis et progressiva	Van Steesel *et al.*, 2009
Cx31	G12D	Erythrokeratodermia variabilis et progressiva	Rouan *et al.*, 2003
	G12R	Erythrokeratodermia variabilis et progressiva	He *et al.*, 2005
	G12S	Erythrokeratodermia variabilis et progressive	Deng *et al.*, 2019
Cx32	G12S	X-linked Charcot-Marie-Tooth disease	Bone *et al.*, 1997; Abrams *et al.*, 2001

Table 2. β-type Connexins (*Homo Sapiens)* Expressed in Skin

Cx	Ref	Nucleotide	Amino acid
26 (GJB2)	NM_004004.6	>NM_004004.6:179-859 Homo sapiens gap junction protein beta 2 (GJB2), mRNA ATGGATTGGGGCACGCTGCAGACGATCCTGGGGGGTGTGAACAAACACTCCACCAGC ATTGGAAAGATCTGGCTCACCGTCCTCTTCATTTTTCGCATTATGATCCTCGTTGTG GCTGCAAAGGAGGTGTGGGGAGATGAGCAGGCCGACTTTGTCTGCAACACCCTGCAG CCAGGCTGCAAGAACGTGTGCTACGATCACTACTTCCCCATCTCCCACATCCGGCTA TGGGCCCTGCAGCTGATCTTCGTGTCCACGCCAGCGCTCCTAGTGGCCATGCACGTG GCCTACCGGAGACATGAGAAGAAGAGGAAGTTCATCAAGGGGGAGATAAAGAGTGAA TTTAAGGACATCGAGGAGATCAAAACCCAGAAGGTCCGCATCGAAGGCTCCCTGTGG TGGACCTACACAAGCAGCATCTTCTTCCGGGTCATCTTCGAAGCCGCCTTCATGTAC GTCTTCTATGTCATGTACGACGGCTTCTCCATGCAGCGGCTGGTGAAGTGCAACGCC TGGCCTTGTCCCAACACTGTGGACTGCTTTGTGTCCCGGCCCACGGAGAAGACTGTC TTCACAGTGTTCATGATTGCAGTGTCTGGAATTTGCATCCTGCTGAATGTCACTGAA TTGTGTTATTTGCTAATTAGATATTGTTCTGGGAAGTCAAAAAAGCCAGTTTAA	>NM_004004.6:179-859 Homo sapiens gap junction protein beta 2 MDWGTLQTILGGVNKHST SIGKIWLTVLFIFRIMIL VVAAKEVWGDEQADFVCN TLQPGCKNVCYDHYFPIS HIRLWALQLIFVSTPALL VAMHVAYRRHEKKRKFIK GEIKSEFKDIEEIKTQKV RIEGSLWWTYTSSIFFRV IFEAAFMYVFYVMYDGFS MQRLVKCNAWPCPNTVDC FVSRPTEKTVFTVFMIAV SGICILLNVTELCYLLIR YCSGKSKKPV
30 (GJB6)	NM_001370090.1	>NM_001370090.1:552-1337 Homo sapiens gap junction protein beta 6 (GJB6), transcript variant 5, mRNA ATGGATTGGGGGACGCTGCACACTTTCATCGGGGGTGTCAACAAACACTCCACCAGC ATCGGGAAGGTGTGGATCACAGTCATCTTTATTTTCCGAGTCATGATCCTCGTGGTG GCTGCCCAGGAAGTGTGGGGTGACGAGCAAGAGGACTTCGTCTGCAACACACTGCAA CCGGGATGCAAAAATGTGTGCTATGACCACTTTTTCCCGGTGTCCCACATCCGGCTG TGGGCCCTCCAGCTGATCTTCGTCTCCACCCCAGCGCTGCTGGTGGCCATGCATGTG GCCTACTACAGGCACGAAACCACTCGCAAGTTCAGGCGAGGAGAGAAGAGGAATGAT TTCAAAGACATAGAGGACATTAAAAAGCAGAAGGTTCGGATAGAGGGGTCGCTGTGG TGGACGTACACCAGCAGCATCTTTTTCCGAATCATCTTTGAAGCAGCCTTTATGTAT GTGTTTTACTTCCTTTACAATGGGTACCACCTGCCCTGGGTGTTGAAATGTGGGATT GACCCCTGCCCCAACCTTGTTGACTGCTTTATTTCTAGGCCAACAGAGAAGACCGTG TTTACCATTTTTATGATTTCTGCGTCTGTGATTTGCATGCTGCTTAACGTGGCAGAG TTGTGCTACCTGCTGCTGAAAGTGTGTTTTAGGAGATCAAAGAGAGCACAGACGCAA AAAAATCACCCCAATCATGCCCTAAAGGAGAGTAAGCAGAATGAAATGAATGAGCTG ATTTCAGATAGTGGTCAAAATGCAATCACAGGTTTCCCAAGCTAA	>NM_001370090.1:552-1337 Homo sapiens gap junction protein beta 6 MDWGTLHTFIGGVNKHST SIGKVWITVIFIFRVMIL VVAAQEVWGDEQEDFVCN TLQPGCKNVCYDHFFPVS HIRLWALQLIFVSTPALL VAMHVAYYRHETTRKFRR GEKRNDFKDIEDIKKQKV RIEGSLWWTYTSSIFFRI IFEAAFMYVFYFLYNGYH LPWVLKCGIDPCPNLVDC FISRPTEKTVFTIFMISA SVICMLLNVAELCYLLLK VCFRRSKRAQTQKNHPNH ALKESKQNEMNELISDSG QNAITGFPS
30.3 (GJB4)	NM_153212.3	>NM_153212.3:372-1172 Homo sapiens gap junction protein beta 4 (GJB4), mRNA ATGAACTGGGCATTTCTGCAGGGCCTGCTGAGTGGCGTGAACAAGTACTCCACAGTG CTGAGCCGCATCTGGCTGTCTGTGGTGTTCATCTTTCGTGTGCTGGTGTACGTGGTG GCAGCGGAGGAGGTGTGGGACGATGAGCAGAAGGACTTTGTCTGCAACACCAAGCAG CCCGGCTGCCCCAACGTCTGCTATGACGAGTTCTTCCCCGTGTCCCACGTGCGCCTC TGGGCCCTACAGCTCATCCTGGTCACGTGCCCCTCACTGCTCGTGGTCATGCACGTG GCCTACCGCGAGGAACGCGAGCGCAAGCACCACCTGAAACACGGGCCCAATGCCCCG TCCCTGTACGACAACCTGAGCAAGAAGCGGGGCGGACTGTGGTGGACGTACTTGCTG AGCCTCATCTTCAAGGCCGCCGTGGATGCTGGCTTCCTCTATATCTTCCACCGCCTC TACAAGGATTATGACATGCCCCGCGTGGTGGCCTGCTCCGTGGAGCCTTGCCCCCAC ACTGTGGACTGTTACATCTCCCGGCCCACGGAGAAGAAGGTCTTCACCTACTTCATG GTGACCACAGCTGCCATCTGCATCCTGCTCAACCTCAGTGAAGTCTTCTACCTGGTG GGCAAGAGGTGCATGGAGATCTTCGGCCCCAGGCACCGGCGGCCTCGGTGCCGGGAA TGCCTACCCGATACGTGCCCACCATATGTCCTCTCCCAGGGAGGGCACCCTGAGGAT GGGAACTCTGTCCTAATGAAGGCTGGGTCGGCCCCAGTGGATGCAGGTGGGTATCCA TAA	>NM_153212.3:372-1172 Homo sapiens gap junction protein beta 4 MNWAFLQGLLSGVNKYST VLSRIWLSVVFIFRVLVY VVAAEEVWDDEQKDFVCN TKQPGCPNVCYDEFFPVS HVRLWALQLILVTCPSLL VVMHVAYREERERKHHLK HGPNAPSLYDNLSKKRGG LWWTYLLSLIFKAAVDAG FLYIFHRLYKDYDMPRVV ACSVEPCPHTVDCYISRP TEKKVFTYFMVTTAAICI LLNLSEVFYLVGKRCMEI FGPRHRRPRCRECLPDTC PPYVLSQGGHPEDGNSVL MKAGSAPVDAGGYP

31 (GJB3)	NM_024009.3	>NM_024009.3:591-1403 Homo sapiens gap junction protein beta 3 (GJB3), transcript variant 1, mRNA ATGGACTGGAAGACACTCCAGGCCCTACTGAGCGGTGTGAACAAGTACTCCACAGCG TTCGGGCGCATCTGCTGTCCGTGGTGTTCGTCTTCCGGGTGCTGGTATACGTGGTGG CTGCAGAGCGCGTGTGGGGGGATGAGCAGAAGGACTTTGACTGCAACACCAAGCAGC CCGGCTGCACCAACGTCTGCTACGACAACTACTTCCCCATCTCCAACATCCGCCTCT GGGCCCTGCAGCTCATCTTCGTCACATGCCCCTCGCTGCTGGTCATCCTGCACGTGG CCTACCGTGAGGAGCGGGAGCGCCGGCACCGCCAGAAACACGGGGACCAGTGCGCCA AGCTGTACGACAACGCAGGCAAGAAGCACGGAGGCCTGTGGTGGACCTACCTGTTCA GCCTCATCTTCAAGCTCATCATTGAGTTCCTCTTCCTCTACCTGCTGCACACTCTCT GGCATGGCTTCAATATGCCGCGCCTGGTGCAGTGTGCCAACGTGGCCCCCTGCCCCA ACATCGTGGACTGCTACATTGCCCGACCTACCGAGAAGAAAATCTTCACCTACTTCA TGGTGGGCGCCTCCGCCGTCTGCATCGTACTCACCATCTGTGAGCTCTGCTACCTCA TCTGCCACAGGGTCCTGCGAGGCCTGCACAAGGACAAGCCTCGAGGGGGTTGCAGCC CCTCGTCCTCCGCCAGCCGAGCTTCCACCTGCCGCTGCCACCACAAGCTGGTGGAGG CTGGGGAGGTGGATCCAGACCCAGGCAATAACAAGCTGCAGGCTTCAGCACCCAACC TGACCCCCATCTGA	>NM_024009.3:591-1403 Homo sapiens gap junction protein beta 3 MDWKTLQALLSGVNKYST AFGRIWLSVVFVFRVLVY VVAAERVWGDEQKDFDCN TKQPGCTNVCYDNYFPIS NIRLWALQLIFVTCPSLL VILHVAYREERERRHRQK HGDQCAKLYDNAGKKHGG LWWTYLFSLIFKLIIEFL FLYLLHTLWHGFNMPRLV QCANVAPCPNIVDCYIAR PTEKKIFTYFMVGASAVC IVLTICELCYLICHRVLR GLHKDKPRGGCSPSSSAS RASTCRCHHKLVEAGEVD PDPGNNKLQASAPNLTPI
31.1 (GJB5)	NM_005268.4	>NM_005268.4:174-995 Homo sapiens gap junction protein beta 5 (GJB5), mRNA ATGAACTGGAGTATCTTTGAGGGACTCCTGAGTGGGGTCAACAAGTACTCCACAGCC TTTGGGCGCATCTGGCTGTCTCTGGTCTTCATCTTCCGCGTGCTGGTGTACCTGGTG ACGGCCGAGCGTGTGTGGAGTGATGACCACAAGGACTTCGACTGCAATACTCGCCAG CCCGGCTGCTCCAACGTCTGCTTTGATGAGTTCTTCCCTGTGTCCCATGTGCGCCTC TGGGCCCTGCAGCTTATCCTGGTGACATGCCCCTCACTGCTCGTGGTCATGCACGTG GCCTACCGGGAGGTTCAGGAGAAGAGGCACCGAGAAGCCCATGGGGAGAACAGTGGG CGCCTCTACCTGAACCCCGGCAAGAAGCGGGGTGGGCTCTGGTGGACATATGTCTGC AGCCTAGTGTTCAAGGCGAGCGTGGACATCGCCTTTCTCTATGTGTTCCACTCATTC TACCCCAAATATATCCTCCCTCCTGTGGTCAAGTGCCACGCAGATCCATGTCCCAAT ATAGTGGACTGCTTCATCTCCAAGCCCTCAGAGAAGAACATTTTCACCCTCTTCATG GTGGCCACAGCTGCCATCTGCATCCTGCTCAACCTCGTGGAGCTCATCTACCTGGTG AGCAAGAGATGCCACGAGTGCCTGGCAGCAAGGAAAGCTCAAGCCATGTGCACAGGT CATCACCCCCACGGTACCACCTCTTCCTGCAAACAAGACGACCTCCTTTCGGGTGAC CTCATCTTTCTGGGCTCAGACAGTCATCCTCCTCTCTTACCAGACCGCCCCCGAGAC CATGTGAAGAAAACCATCTTGTGA	>NM_005268.4:174-995 Homo sapiens gap junction protein beta 5 (GJB5) MNWSIFEGLLSGVNKYST AFGRIWLSLVFIFRVLVY LVTAERVWSDDHKDFDCN TRQPGCSNVCFDEFFPVS HVRLWALQLILVTCPSLL VVMHVAYREVQEKRHREA HGENSGRLYLNPGKKRGG LWWTYVCSLVFKASVDIA FLYVFHSFYPKYILPPVV KCHADPCPNIVDCFISKP SEKNIFTLFMVATAAICI LLNLVELIYLVSKRCHEC LAARKAQAMCTGHHPHGT TSSCKQDDLLSGDLIFLG SDSHPPLLPDRPRDHVKK TIL
32 (GJB1)	NM_001097642	>NM_001097642.2:96-947 Homo sapiens gap junction protein beta 1 (GJB1), transcript variant 1, mRNA ATGAACTGGACAGGTTTGTACACCTTGCTCAGTGGCGTGAACCGGCATTCTACTGCC ATTGGCCGAGTATGGCTCTCGGTCATCTTCATCTTCAGAATCATGGTGCTGGTGGTG GCTGCAGAGAGTGTGTGGGGTGATGAGAAATCTTCCTTCATCTGCAACACACTCCAG CCTGGCTGCAACAGCGTTTGCTATGACCAATTCTTCCCCATCTCCCATGTGCGGCTG TGGTCCCTGCAGCTCATCCTAGTTTCCACCCCAGCTCTCCTCGTGGCCATGCACGTG GCTCACCAGCAACACATAGAGAAGAAAATGCTACGGCTTGAGGGCCATGGGGACCCC CTACACCTGGAGGAGGTGAAGAGGCACAAGGTCCACATCTCAGGGACACTGTGGTGG ACCTATGTCATCAGCGTGGTGTTCCGGCTGTTGTTTGAGGCCGTCTTCATGTATGTC TTTTATCTGCTCTACCCTGGCTATGCCATGGTGCGGCTGGTCAAGTGCGACGTCTAC CCCTGCCCCAACACAGTGGACTGCTTCGTGTCCCGCCCCACCGAGAAAACCGTCTTC ACCGTCTTCATGCTAGCTGCCTCTGGCATCTGCATCATCCTCAATGTGGCCGAGGTG GTGTACCTCATCATCCGGGCCTGTGCCCGCCGAGCCCAGCGCCGCTCCAATCCACCT TCCCGCAAGGGCTCGGGCTTCGGCCACCGCCTCTCACCTGAATACAAGCAGAATGAG ATCAACAAGCTGCTGAGTGAGCAGGATGGCTCCCTGAAAGACATACTGCGCCGCAGC CCTGGCACCGGGGCTGGGCTGGCTGAAAAGAGCGACCGCTGCTCGGCCTGCTGA	M>NM_001097642.2:96-947 Homo sapiens gap junction protein beta 1 MNWTGLYTLLSGVNRHST AIGRVWLSVIFIFRIMVL VVAAESVWGDEKSSFICN TLQPGCNSVCYDQFFPIS HVRLWSLQLILVSTPALL VAMHVAHQQHIEKKMLRL EGHGDPLHLEEVKRHKVH ISGTLWWTYVISVVFRLL FEAVFMYVFYLLYPGYAM VRLVKCDVYPCPNTVDCF VSRPTEKTVFTVFMLAAS GICIILNVAEVVYLIIRA CARRAQRRSNPPSRKGSG FGHRLSPEYKQNEINKLL SEQDGSLKDILRRSPGTG AGLAEKSDRCSAC

Table 3. Connexin Constucts and Molecular Biology of Mutagenesis

Connexin	**Species**	**Vector**	**Restriction enzyme ***	**Priming site RNA Pol**	**Gift from**
Cx31	human	pcDNA	Xho1	T7	*David Kelsell*
Cx32	Rat	pGem7zf+	Xba1	SP6	*Bruce Nicholson*

- linearizes downstream of the connexin gene

FIGURES

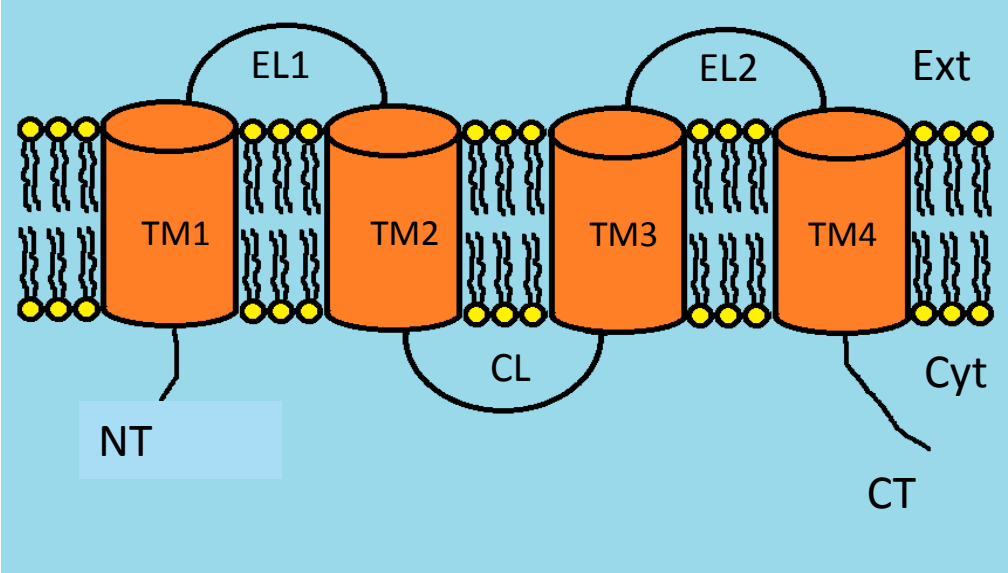

Figure 1. Connexin topology showing amino terminus (NT), cytoplasmic loop (CL) and cytoplasmic terminus (CT) on the cytoplasmic side of the membrane. Connexins also have four transmembrane domains (TM1-TM4) and two extracellular loops (EL1, EL2). Handrawn

A

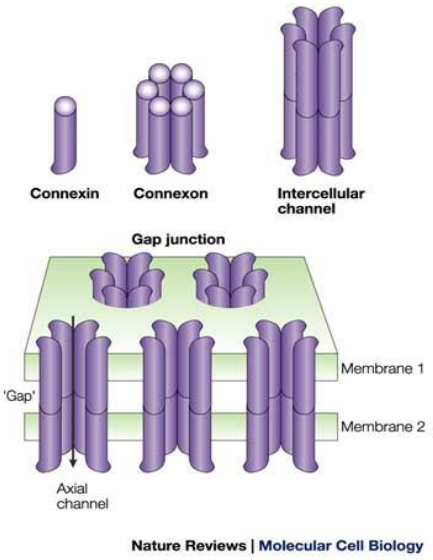

B

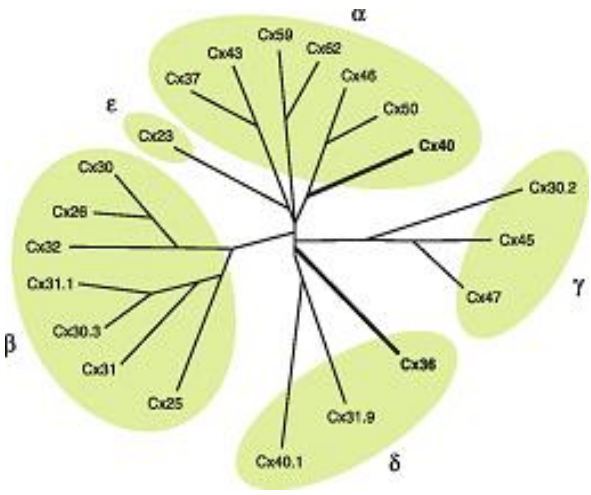

Figure 2. A) Illustration of connexin oligomerize to form connexons (also known as hemichannels) and intercellular channels (gap junction channels). Six connexins oligomerize around a central pore to form a connexon. An intercellular channel is formed when two connexons dock together (from Goodenough and Paul, 2003). B) Grouping of connexins into families is dependent on sequence, and can provide a basis for anticipated interactions. Connexins targeted in this study lie within the beta-family (ß) and are expected to interact heteromerically and heterotypically (from Bosco *et al.*, 2011)

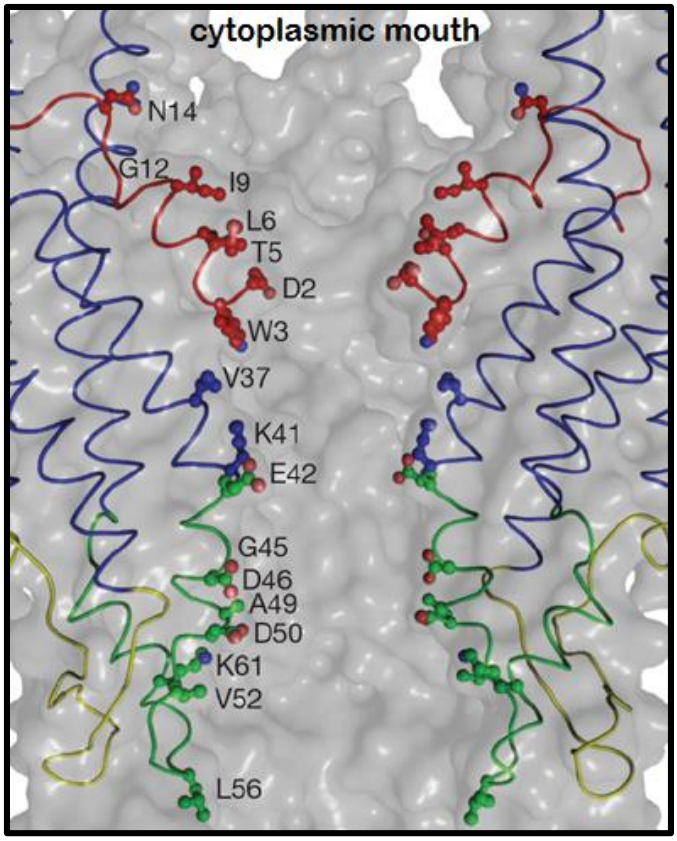

Figure 3. Structure of a Cx26 gap junction channel pore with selected amino acids labelled. Cytoplasmic face is top where the pore is widened. Only half of a channel is shown in this image Relevant to this study is the position of G12 which resides near a bend in the amino terminus (NT, red). NT folds into the pore and interacts closely with the first transmembrane domain (TM1). Transmembrane domains are shown in blue and extracellular loops are green. (from Maeda *et al*., 2009).

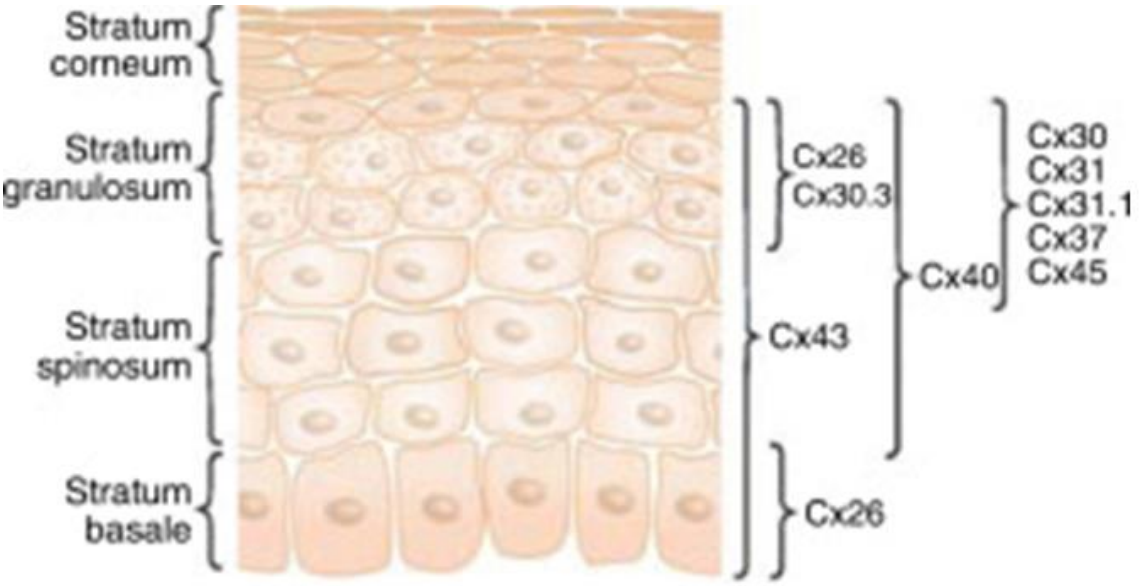

Figure 4. Illustration of human skin showing distinct layers that develop as cells progress and differentiate from the basale to the corneal layers. At least nine connexins are expressed in skin in specific but overlapping patterns. The beta-type connexins Cx26, Cx30, Cx30.3, Cx31 are co-expressed in the stratum granulosom. Cx32 is also expressed at low levels in the granular layer of palmar skin (Di *et al.,* 2005). (image from Mese *et al*., 2007)

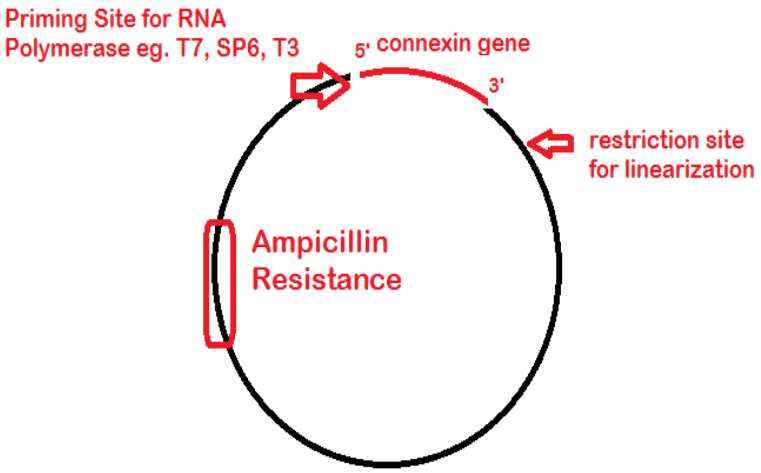

Figure 5. Vectors used for connexin expression in oocytes include several standard features. Although the connexin genes have been subcloned into a variety of different vectors each vector includes sequences for selection which in all cases conferred ampicillin resistance, a promoter for RNA polymerase that is located upstream of the 5' region of the connexin gene (eg. T7, SP6 or T3) and a restriction site used to linearize the plasmid downstream of the 3' end of the gene prior to *in vitro* transcription.

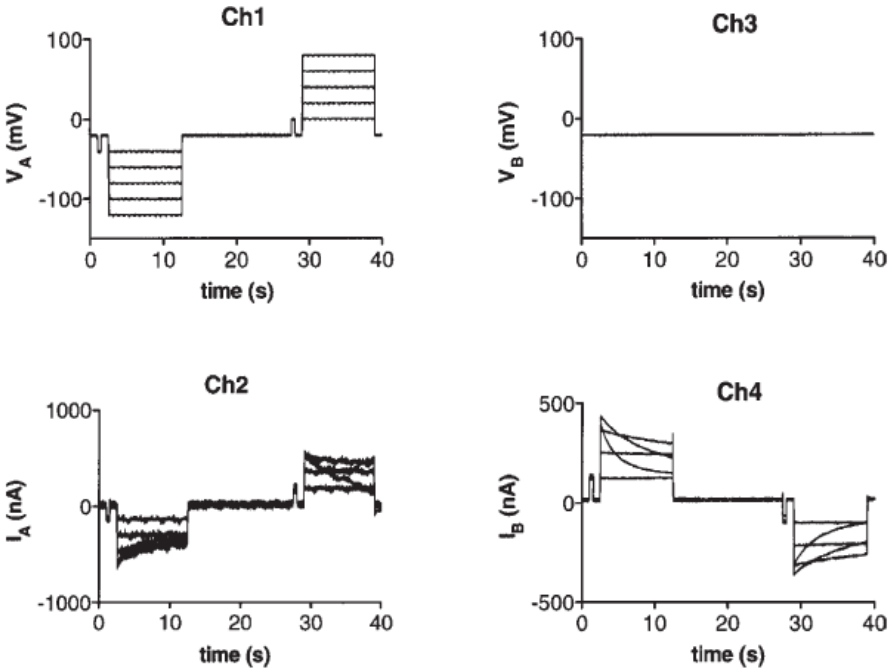

Figure 6. Example of four channels recorded during dual cell two-electrode voltage clamp. Voltage is clamped in both cells and current is recorded. Voltage is controlled by an amplifier and computer program. Junctional currents are recorded from the cell that is clamped at a constant voltage while voltage in the adjacent cell is changed. In this configuration the only voltage gradient induced in that cell occurs across the junction. TOP LEFT: voltage in the pulsed cell. TOP RIGHT: voltage in the clamped cell often involves a series of voltage steps to induce progressively higher voltages across the junction. A small pre-pulse is often included to demonstrate stability of the recording. BOTTOM LEFT: current in the pulsed cell (combination of junctional and transmembrane currents). BOTTOM RIGHT: current in the clamped cell (junctional current). Junctional currents decay in time- and voltage-dependent manner (from Skerrett *et al.*, 2001)

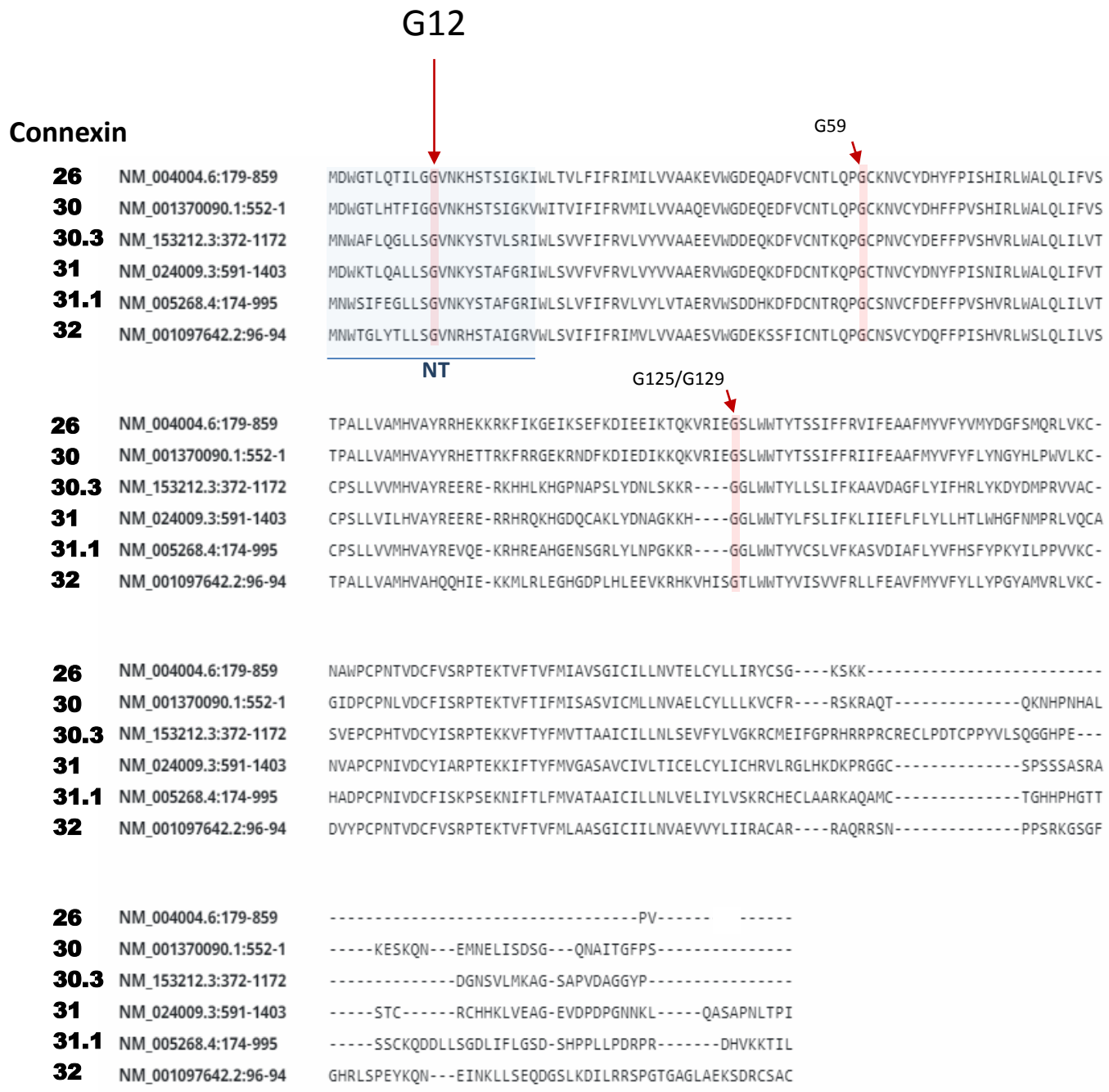

Figure 7. Amino acid alignment of five beta-type connexins expressed in human skin. Conserved glycine residues are highlighted in red and the amino terminus is shaded blue. Sequences were aligned using Clustal (MPI Bioinformatics Tools).

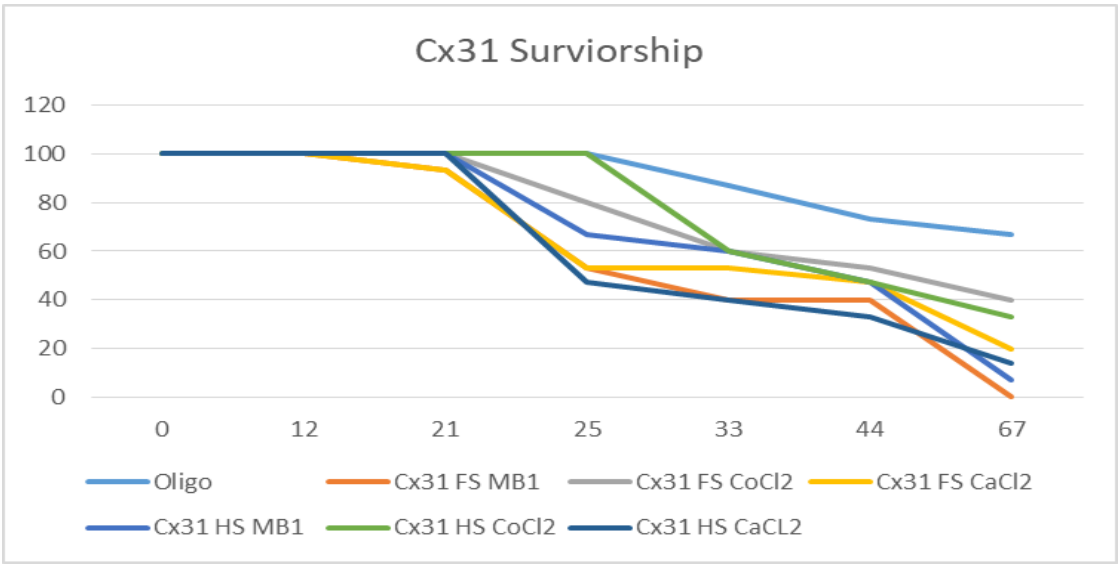

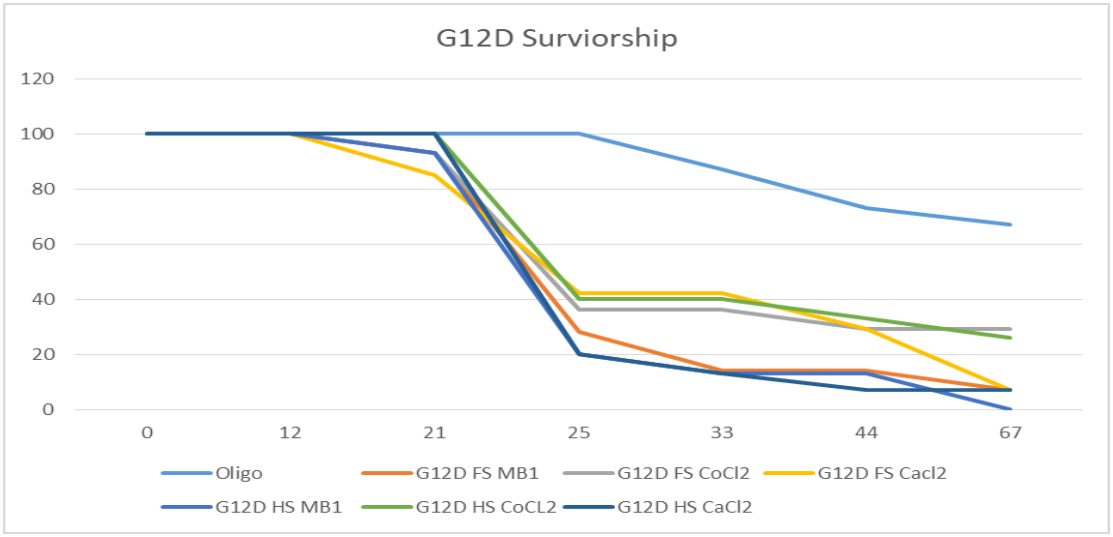

.

Figure 8. Oocyte survival after injection of RNA encoding Cx31 (top) or Cx31G12D (bottom). After injection of RNA oocytes was observed for 72 hours and the percentage of surviving oocytes was plotted. Approximately 15 oocytes were included in each group. Negative control is "oligo" indicating that oocytes received only morpholino against XeCx38. Media bathing the oocytes included MBI alone or supplemented with calcium ($CaCl_2$, 2 mM) and cobalt ($CoCl_2$ 1 mM). In addition RNA was tested at 125 ng/ul (about 5 nm per oocyte, FS) and 65 ng/ul (about 2.5 ng per oocyte HS)

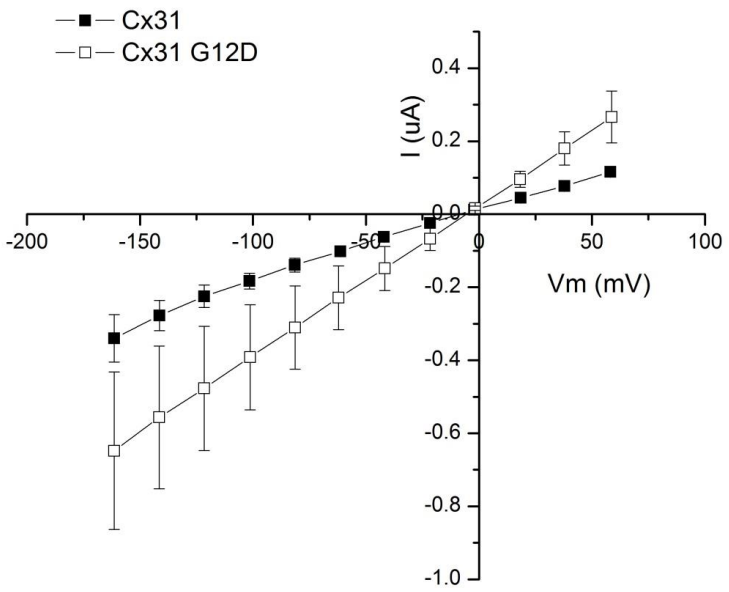

Figure 9. Cx31G12D induces membrane currents in single oocytes. Current versus voltage plots for Cx31G12D and wildtype Cx31 demonstrate that the mutant G12D increases membrane permeability. Currents were induced by voltage pulses from a holding potential of -20 mV to +60 and then -160 mV in 20 mV increments. N = 3.

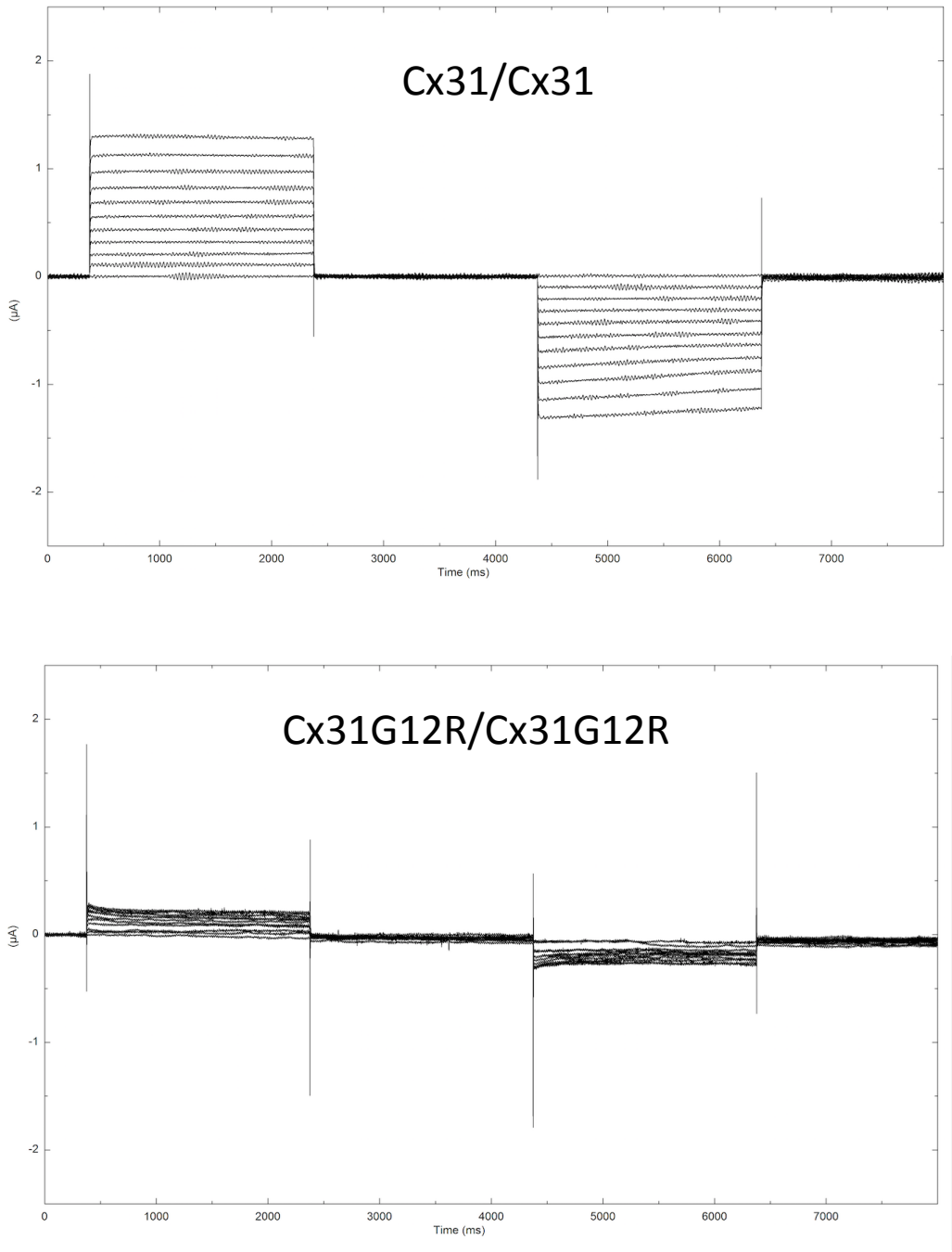

Figure 10. Gap junction intercellular currents recorded from paired *Xenopus* oocytes expressing Cx31 (TOP) or Cx31G12R (LOWER). After injection of RNA (125 ng/ul) the vitelline layers were removed and oocytes were paired overnight. Currents were recorded in a continuously clamped oocyte while its partner was pulsed in 20 mV increments to induce Vj's up to +100 mV and -100 mV. Data was collected by Adedoyin Akingbade who was an undergraduate student working under my guidance at the time of the recordings.

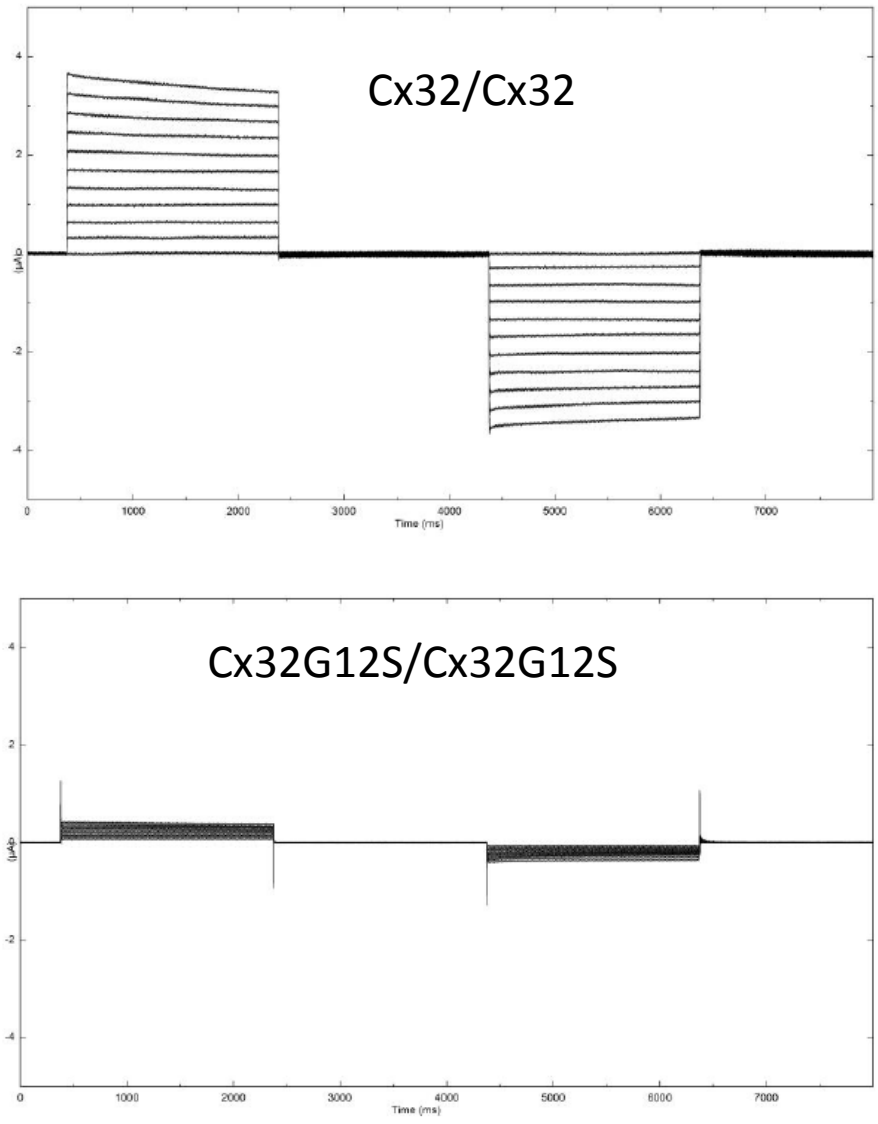

Figure 11. Gap junction intercellular currents recorded from paired *Xenopus* oocytes expressing Cx32 (TOP) or Cx32G12S (LOWER). After injection of RNA (125 ng/ul) the vitelline layers were removed and oocytes were paired overnight. Currents were recorded in a continuously clamped oocyte while its partner was pulsed in 20 mV increments to induce Vj's up to +100 mV and -100 mV.